UDC 534.21-8:[537.226.83:537.311.322]:546.681'19
Electronics and Communications in Japan, Part 2, Vol. 68, No. 6, 1985
Translated from Denshi Tsushin Gakkai Ronbunshi, Vol. 68-C, No. 2, February 1985, pp. 101-108

Analyses and Experiments of Nonlinear Phenomena in Piezoelectric Semiconductors

Kazuhiko Yamanouchi, Member, and Tsutomu Inada, Nonmember

Research Institute of Electrical Communication, Tohoku University, Sendai, Japan 980

SUMMARY

Since a GaAs semiconductor has a piezoelectricity and a high mobility at the same time, it has attracted the attention of many research workers as material for surface-acoustic-wave (SAW) devices utilizing its nonlinearity. However, in published works, the analyses have regarded a semiconductor substrate as a piezoelectric element, or an epitaxial-growth film as a semiconductor. Also, some analyses of a piezoelectric semiconductor were limited to a one-dimensional model, or to obtaining the velocity and attenuation of the surface wave by using the perturbation method.

In this paper, a numerical analysis of the SAW on a general piezoelectric element is carried out. The propagation characteristics of the SAW for the carrier density of a semiconductor, the convolution efficiency for the carrier density, and its dependence on the mobility represent new findings. Also, the results of analyses on a double-layer are shown. Also, the experimental results of the excitation characteristics of an SAW on a GaAs piezoelectric element, and the output of the convolution relating to the carrier density are shown.

1. Introduction

A surface acoustic wave (SAW) is a wave in which most of the energy propagates in concentration within the depth of the layer less than one wavelength. Therefore, the wave can easily be controlled from the surface. Since this is an elastic wave, its propagation velocity is as small as about 10^{-5} of an electromagnetic wave. Thus, a device using this type of wave can be designed smaller and lighter. When a piezoelectric medium is used for this type of wave, an electric field is generated by the propagation of the wave. By using these features, various devices using an SAW can be designed. Notably, nonlinear devices having various structures, such as a convolver and correlator, have been studied by utilizing the interaction of the electric field of an SAW and the carrier of a semiconductor [1].

Since GaAs belonging to point group $43m$ is a semiconductor having a piezoelectricity, and its electric field due to an SAW and semiconductor carriers interact strongly, this has recently been used as a substrate of SAW devices [2]. The analysis of GaAs for its application to an SAW device as a piezoelectric semiconductor, however, has almost been disregarded. In most published research, the semiconductor carriers in a substrate are ignored in the analysis of the piezoelectric material; or the piezoelectricity is ignored in the analysis of a semiconductor when, for example, epitaxial-growth film is used. In some investigations which consider both piezoelectricity and semiconductor carriers for a piezoelectric semiconductor, the analysis of an SAW propagation in an arbitrary direction has not been carried out, although they contain the deduction as the velocity and attenuation of bulk wave in a one-dimensional model [3], and those in a particular crystal and in a particular direction by using the perturbation method [4].

In this paper, a general analytical method for SAWs in a piezoelectric semiconductor is expanded, so that a numerical analysis method is obtained which can be applied generally to piezoelectric semiconductors. Calculation of an actual GaAs crystal was carried out, and the variations of the propagation characteristic of an SAW due to some parameters (e.g., the carrier density and the mobility) were found. By using the distribution of displacements of an SAW and that

ISSN8756-663X/85/0006-0048$7.50/0

of the electric potential (which are obtained from the analysis), the analysis of the convolver was carried out using a nonlinear current model, and the figure of merit was obtained. As a result, it was found that GaAs has a rather large figure of merit in an appropriate carrier density, despite its small electromechanical coupling coefficient K^2. Assuming a structure of a GaAs semiconductor substrate with epitaxial-growth film, a similar numerical analysis was carried out for a double-layer structure consisting of a piezoelectric semiconductor on another piezoelectric element, and the propagation characteristics (e.g., the velocity and attenuation of an SAW) were obtained. The figure of merit for the double-layer structure piezoelectric semiconductor in the use of a convolver was obtained, with the variation of this figure due to the change of the parameters (e.g., the thickness of the layer).

The contents of this paper are as follows: In section 2, the theoretical analysis is described. The propagation characteristic of the SAW in a piezoelectric semiconductor, and the method of numerical analysis of the figure of merit of the convolver are shown taking a single- and double-layer structure. The results of the numerical analysis for an actual GaAs device are shown.

In section 3, the making of the convolver using a GaAs substrate and its experiment are described, together with comparison with the theoretical analysis.

2. Propagation Characteristics of an SAW in a Piezoelectric Semiconductor and the Analysis of a Convolver

This section describes a method for analyzing the propagation characteristics of an SAW for a piezoelectric semiconductor substrate, and a method for analyzing the figure of merit of a convolver, together with their results.

2.1 Propagation characteristics of an SAW in a piezoelectric semiconductor

Let the direction perpendicular to the surface of a piezoelectric semiconductor be the x_2-axis, the direction of propagation of an SAW be the x_1 axis, and the axis perpendicular to the x_1 axis be the x_3-axis. Also, let the propagation velocity of the SAW be v, and the attenuation constant in the propagation direction be δ. As a general piezoelectric material, the displacement of the SAW, u_1, u_2 and u_3, and the electric potential ϕ of the wave are given by the following set of equations:

$$\left.\begin{aligned} u_1 &= \alpha_1 \exp \Omega k x_2 \exp j k (\ell x_1 - v t) \\ u_2 &= \alpha_2 \exp \Omega k x_2 \exp j k (\ell x_1 - v t) \\ u_3 &= \alpha_3 \exp \Omega k x_2 \exp j k (\ell x_1 - v t) \\ \phi &= \alpha_4 \exp \Omega k x_2 \exp j k (\ell x_1 - v t) \end{aligned}\right\} \quad (1)$$

where k is the wave number, Ω is the attenuation constant in the direction of the depth ($-x_2$ direction), $\ell = 1 + j\delta$ and α_1 to α_4 are unknown constants. The fundamental equations of the piezoelectric semiconductor become as follows:

$$\left.\begin{aligned} &\left.\begin{aligned} \boldsymbol{T} &= \boldsymbol{C}^E : \boldsymbol{S} - \boldsymbol{e} \cdot \boldsymbol{E} \\ \boldsymbol{D} &= \boldsymbol{e} : \boldsymbol{S} + \epsilon^S \cdot \boldsymbol{E} \end{aligned}\right\} \text{equations for piezoelectricity} \\ &\nabla \cdot \boldsymbol{D} = q' \qquad \text{Poisson's equation} \\ &\nabla \cdot \boldsymbol{T} = \rho \frac{\partial^2 \boldsymbol{u}}{\partial t^2} \qquad \text{equation of motion} \\ &\nabla \cdot \boldsymbol{J} + \frac{\partial q}{\partial t} = 0 \qquad \text{current-continuity eq.} \\ &\boldsymbol{J} = \mu q \boldsymbol{E} - D \nabla q \qquad \text{equation for current in semiconductor} \\ &\boldsymbol{E} = -\nabla \phi \qquad \text{quasi-electrostatic approximation} \end{aligned}\right\} \quad (2)$$

where T is the stress, D is the electric flux density, S is the strain, E is the electric field, $q = q_0 + q'$ is the electric charge density, q' being the variation due to the SAW, ρ is the density of mass, D is a diffusion constant. Since the propagation velocity of the SAW is much smaller than that of the electromagnetic wave, a quasielectrostatic approximation is used. Considering only the electrons as the semiconductor carriers, the Einstein relationship is applied between the mobility and the diffusion constant. By using the above-described fundamental equations, the semiconductor equations for α_1, α_2, α_3 and α_4 are obtained.

By putting the coefficient matrix equations of these semiconductor equations to zero, the 10th-order equation for Ω is obtained. By solving this 10th-order equation, five values of Ω whose real parts are positive are used. Letting them be $\Omega(1)$, $\Omega(2)$, ..., $\Omega(5)$, let the ratios of α_1, α_2, α_3 and α_4 to each $\Omega(i)$ be $\alpha_m(i)$. The general solution of the displacement and electrical potential of the SAW become a linear sum of these five values. Letting the coupling coefficient be $A(i)$, the following equations are obtained:

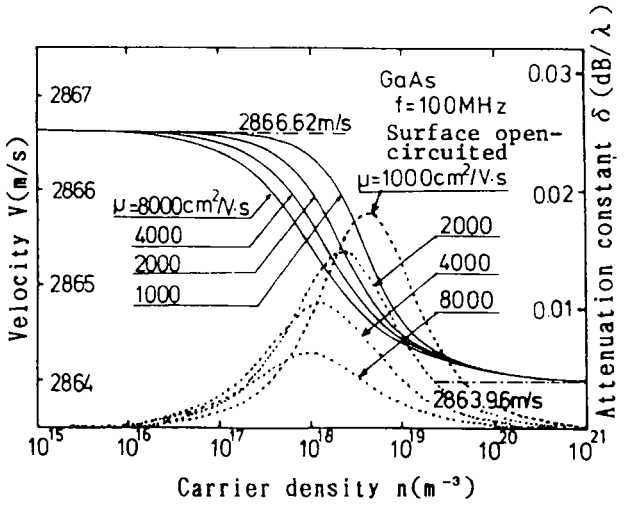

GaAs (Surface open), — Velocity, ··· Attenuation

Fig. 1. Propagation characteristics of SAW on ⟨100⟩, (011).

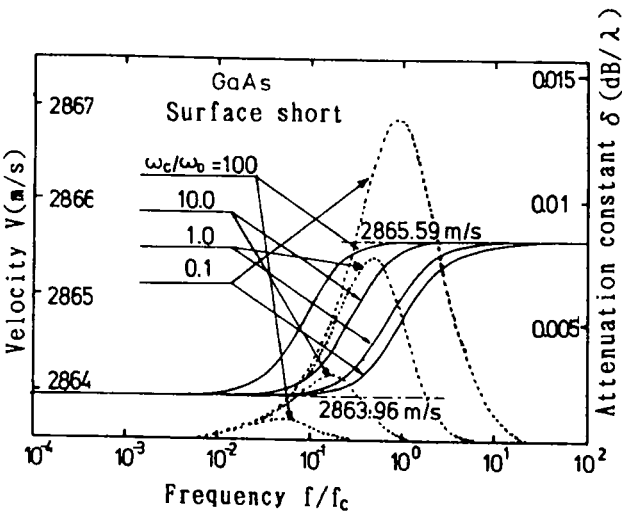

GaAs (Surface short), —Velocity, ··· Attenuation

Fig. 2. Propagation characteristics of SAW on ⟨100⟩, (011).

$$\left.\begin{aligned} u_1 &= \sum_{i=1}^{5} A(i)\alpha_1(i)\exp\Omega(i)kx_2\exp j k(lx_1-vt) \\ u_2 &= \sum_{i=1}^{5} A(i)\alpha_2(i)\exp\Omega(i)kx_2\exp j k(lx_1-vt) \\ u_3 &= \sum_{i=1}^{5} A(i)\alpha_3(i)\exp\Omega(i)kx_2\exp j k(lx_1-vt) \\ \phi &= \sum_{i=1}^{5} A(i)\alpha_4(i)\exp\Omega(i)kx_2\exp j k(lx_1-vt) \end{aligned}\right\} \quad (3)$$

When this general solution satisfies the boundary condition, the solution for the SAW is given.

Next, the boundary conditions are considered. The electric potential in a vacuum ϕ_V is assumed as follows:

$$\phi_V = A\exp\beta x_2 \cdot \exp j k(lx_1-vt) \quad (4)$$

β is obtained from the Laplace equation:

$$\begin{aligned}\phi_V = &(A'\exp klx_2 + B'\exp(-klx_2)) \\ &\cdot\exp j k(lx_1-vt)\end{aligned} \quad (5)$$

From $x_2 = 0$ at $\phi = \phi_V$, and $x_2 = h$ which is a gap between the surface of the substrate and the perfect conductor at $\phi_V = 0$, A' and B' are obtained. The electric potential in the vacuum ϕ_V becomes as follows:

$$\phi_V = \sum_{i=1}^{5} A(i)\alpha_4(i)\frac{\sinh kl(h-x_2)}{\sinh klh}\exp j k(lx_1-vt) \quad (6)$$

Then the electric field in the vacuum and the electric flux density are obtained.

Since the stress is zero at the surface $x_2 = 0$,

$$T_2|_{x_2=0} = T_4|_{x_2=0} = T_6|_{x_2=0} = 0 \quad (7)$$

From the continuity of the current,

$$J_2|_{x_2=0} = 0 \quad (8)$$

From the continuity of the vertical component of the electric flux,

$$D_2|_{x_2=0} = D_{air_2}|_{x_2=0} \quad (8')$$

Under these conditions, let the gap between the surface substrate and a perfect conductor be $h \to \infty$ when the surface ($x_2 = 0$) is electrically open; and $h \to 0$ when it is short-circuited.

When the preceding five boundary conditions are used, a set of 5th order semiconductor equations for coefficient $A(i)$ is obtained.

If the propagation velocity and attenuation of the wave assumed initially is the same as those of the actual wave, the coefficient matrix equation of the simultaneous

equations become zero. In a numerical computation, the coefficient matrix equations are computed successively with various propagation velocities and attenuations until the equations become zero. The final values of the propagation velocity and attenuation are taken as the solution of the SAW.

The distribution of displacements are obtained by giving the ratio of $A(i)$ first, then substituting this into Eq. (3). The Leaky SAW is obtained by changing the method of choosing the Ω from five values.

The results of the numerical analysis of the propagation characteristics of the SAW in a GaAs piezoelectric semiconductor are described next.

Figures 1 and 2 show the propagation characteristics of the SAW on $\langle 100 \rangle$ surface and (011) direction obtained from the numerical computation on the above-described analytical method. The electromechanical coupling coefficient K^2 is about 0.07%, when the GaAs is regarded as a piezoelectricity in the cut and propagation direction chosen. This value is large as a GaAs [2]. The branch of the Rayleigh wave in this cut and propagation direction is degenerated into a slow bulk transversal wave. The SAW whose propagation velocity is calculated as above is a branch of the Leaky SAW. In $\langle 100 \rangle$ surface and (011) propagation, however, a bulk wave (a slow transversal wave), which is slower than the propagation velocity of the SAW and causes the Leaky SAW, does not couple with the SAW, and becomes a SAW without decaying.

Figure 1 shows the dependency of the velocity and attenuation of the SAW on the carrier density, when the surface of the GaAs is open-circuited. In a region where the carrier density is low, the velocity is similar to the velocity calculated for a GaAs piezoelectric substrate alone (2866.62 m/s for the surface which is open-circuited), since the electric field due to the piezoelectric effect remains. In a region where the carrier density is high, the velocity is closed to the velocity obtained for a zero piezoelectric constant (2863.96 m/s, the value for an assumption that GaAs is a plain elastic body), since the electric field due to the piezoelectricity is immediately short-circuited by the carriers. When the value of the mobility increases, the carrier density which changes the propagation velocity changes considerably. The greater the carrier density is, the greater the propagation velocity changes even with a small carrier density, since the effect of the short-circuiting of the electric field (due to the piezoelectric effect) is great. The attenuation has a peak in the transient region

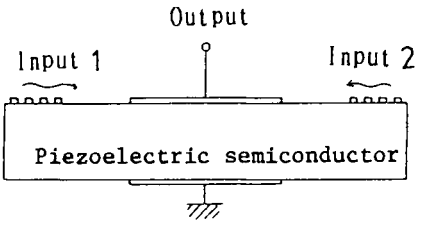

Fig. 3. Configuration of convolver.

where the propagation velocity changes. It is considered that an interaction of the SAW and the semiconductor carriers occurs in this region.

Figure 2 shows the frequency dependence of the propagation velocity and attenuation of the SAW. The frequency on the horizontal axis is normalized by referring to the dielectric relaxation frequency $f_c (2\pi f_c = \omega_c = \sigma/E)$ and ω_c/ω_D is taken as a parameter; ω_D is the diffusion frequency $(\omega_D = v^2/D = ev^2/\mu kT)$. When ω_c/ω_D is constant, the mobility μ and the carrier density n are not uniquely determined, but $n\mu^2$ becomes constant. The numerical computation using this condition shows that the same velocity and the same attenuation are obtained for f/f_0. Reference [3] describes the velocity and attenuation becoming the functions of ω_c/ω_D and ω/ω_c, respectively, in a one-dimensional model. It is confirmed in this paper that this can be applied to the SAW. When the electromechanical coupling coefficient K^2 is large and the velocity changes greatly with the change of the frequency, however, ω_D changes due to the change of the velocity. As a result, the above-described conditions are no longer maintained. The electromechanical coupling coefficient K^2 of the GaAs used for the above computation has a small value, and the change of the propagation of the SAW is small; the parameter in the one-dimensional model could be applied.

2.2 Analysis of a convolver using a nonlinear current model

For section 2.1, the distribution of displacements and electric potential of an SAW propagating on the surface of a piezoelectric semiconductor can be analyzed. Nonlinear current J_n can be obtained from this, and then a convolver having J_n as its source is analyzed. To consider a convolver as shown in Fig. 3, a nonlinear current for a case where two SAWs propagate in opposite

Table 1. Comparison of piezoelectric semiconductor convolvers

	Carrier mobility μ ($cm^2/V\cdot s$)	Carrier density n (m^{-3})	Figure of merit M ($V\cdot m/W$)	Attenuation constant δ (dB/cm)
GaAs	4000	1.6×10^{18}	0.048	2.2×10^{0}
CdS	350	1.0×10^{19}	0.11	1.5×10^{2}
ZnO	180	1.7×10^{19}	0.30	2.0×10^{2}
InSb	100000	1.9×10^{19}	0.017	1.9×10^{-3}

directions is obtained. The density of charge and the electric field in this case are given by

$$\left.\begin{aligned} q' &= q_1\cos(\omega t-kx_1)+q_2\cos(\omega t+kx_1) \\ \boldsymbol{E}' &= \boldsymbol{E}_1\cos(\omega t-kx_1)+\boldsymbol{E}_2\cos(\omega t+kx_1) \end{aligned}\right\} \quad (9)$$

where the subscripts 1 and 2 show input 1 and input 2, and the direction of the wave propagation is x_1. The nonlinear current J_n becomes [5]

$$\begin{aligned} \boldsymbol{J}_n &= \mu q'\boldsymbol{E}' \\ &= \frac{1}{2}\mu(q_1\boldsymbol{E}_1+q_2\boldsymbol{E}_2)+\frac{1}{2}\mu q_1\boldsymbol{E}_1\cos 2(\omega t-kx_1) \\ &\quad +\frac{1}{2}\mu q_2\boldsymbol{E}_2\cos 2(\omega t+kx_1)+\frac{1}{2}\mu(q_1\boldsymbol{E}_2+q_2\boldsymbol{E}_1) \\ &\quad \cdot\cos 2\omega t+\frac{1}{2}\mu(q_1\boldsymbol{E}_2+q_2\boldsymbol{E}_1)\cos 2kx_1 \end{aligned} \quad (10)$$

Since the configuration of the convolver is considered as shown in Fig. 3, the fourth term in J_n is taken which oscillates with 2ω and independent of x_1. It is considered then that a nonlinear field occurs due to this nonlinear current. In the remainder of the paper, the nonlinear current is represented by the following complex form:

$$\boldsymbol{J}_n=\frac{1}{2}\mu(q_1\boldsymbol{E}_2+q_2\boldsymbol{E}_1)\exp(-j2\omega t) \quad (11)$$

It is considered that the nonlinear field having J_n as the course also varies with $\exp(-j\,2\omega t)$. The equation of the current in the semiconductor, including J_n, is expressed by the following equation:

$$\boldsymbol{J}=\sigma\boldsymbol{E}'-D\nabla q+\boldsymbol{J}_n \quad (12)$$

The differential equation satisfying the potential ϕ_n of the nonlinear field is derived from Eq. (2) [the basic equation] and Eq. (12) as follows:

$$\left(\frac{\partial^2}{\partial x_2^2}-K_0^2\right)\frac{\partial^2}{\partial x_2^2}\phi_n=-\frac{1}{D\epsilon^s_{22}}\frac{\partial}{\partial x_2}J_{n2} \quad (13)$$

where $K_0^2=\dfrac{\sigma}{D\epsilon^s_{22}}(1-2\eta)$, $\eta=j\dfrac{\omega}{\omega_c}$, $\omega_c=\dfrac{\sigma}{\epsilon^s_{22}}$

J_{n2} is the x_2-direction component of J_n, the nonlinear strain and stress due to the nonlinear current are negligible, and x_2 is the direction perpendicular to the substrate. By solving Eq. (13), ϕ_n is obtained as follows:

$$\phi_n=\phi_0+\phi_1x_2+\phi_2\exp(-K_0x_2)+\phi_3\exp(K_0x_2)+\Phi \quad (14)$$

where ϕ_c, ϕ_1, ϕ_2 and ϕ_3 are undetermined constants, and Φ is a particular solution derived from J_{n2}.

The undetermined constants in Eq. (14) can be obtained from the boundaries. The boundary conditions for the upper and lower surfaces of the convolver substrate are

$$\left.\begin{aligned} J_{n2}|_{x_2=0} &= J_{n2}|_{x_2=-h}=0 \\ E_{n2}|_{x_2=0} &= E_{n2}|_{x_2=-h}=0 \\ \phi_n|_{x_2=-h} &= 0 \end{aligned}\right\} \quad (15)$$

where h is the thickness of the substrate, and the open output voltage is considered. The undetermined constants are obtained by the electric field and current distribution from Eq. (14), and by substituting them into Eq. (15); then the potential of the nonlinear field ϕ_n is determined. When ϕ_n is obtained, the output voltage of the convolver V_{out} is obtained from the voltage difference between

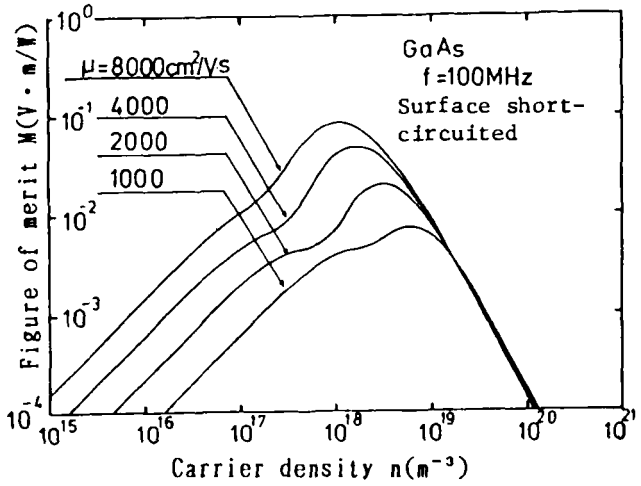

Fig. 4. Figure of merit of GaAs convolver vs. carrier density with mobilities as a parameter.

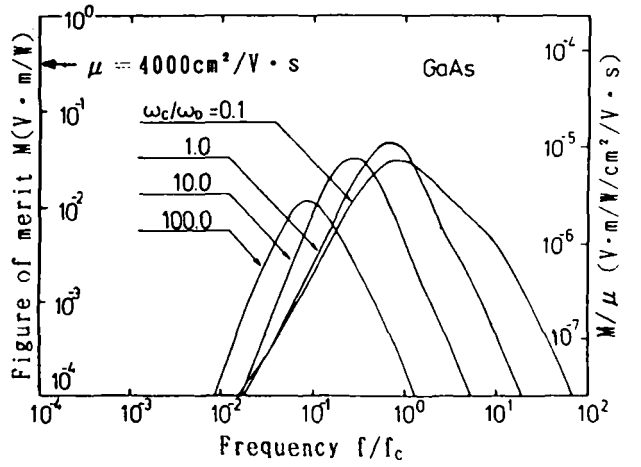

Fig. 5. Figure of merit vs. frequency with ω_c/ω_D as a parameter.

the upper and lower substrates of the convolver.

Letting the power of the SAWs coming from the left and right be P_1 and P_2, respectively, the figure of merit of the convolver M is defined by the following equation:

$$M=\frac{V_{out}(\mathrm{rms})}{\sqrt{P_1\cdot P_2}} \tag{16}$$

The input power is obtained by integrating the potential vector of the SAW, as shown in the following equation, in the direction of the depth:

$$P=-\frac{\dot{u}^*\cdot T}{2}+\frac{\phi\cdot\dot{D}^*}{2}+\frac{\phi\cdot J^*}{2} \tag{17}$$

In the actual numerical analysis of the figure of merit M, the analysis of the velocity and attenuation of an SAW is carried out first, and the distributions of the displacement and electric potential are obtained. Then V_{out}, P_1 and P_2 are computed.

Table 1 shows the figure of merit M of the convolver using known typical piezoelectric semiconductors. CdS and ZnO show higher values of M than GaAs, but they are not useful in practice since the attenuations of their SAW are large. InSb is also not

practical although this has a small attenuation, since this has a low piezoelectricity and small value of M, and a small band gap causes a thermal instability. Comparing them, GaAs has a large M, a small attenuation, a large band gap and a thermal stability. Therefore, this is considered to be the best among the known piezoelectric semiconductors.

Figures 4 and 5 show the details of numerical computations of the figure of merit M for GaAs using the mobility and frequency as parameters. Figure 4 shows the dependence of M on the carrier density, taking the mobility μ as a parameter. When the carrier is small, the greater the M, since the electric field due to the piezoelectricity is almost constant independent of the mobility. When the carrier is large, the value of M becomes small independent of the mobility, since the electric field due to the piezoelectricity is short-circuited by the carriers, and the electric field generated becomes small.

Figure 5 shows the dependence of the value of M on the frequency taking ω_c/ω_D as a parameter. At a low frequency, the value of M becomes small since the effect of the short-circuiting of the electric field due to the carriers is great. At a high frequency, the value of M again becomes small, since the response of the carriers to the SAW becomes poor. In section 2.1, the propagation velocity and attenuation, taking ω_c/ω_D, as a parameter, was constant. However, the value of M varies since this is related to J_n; J_n changes proportionally to μ, even if with a mobility μ and carrier density n for a constant value of ω_c/ω_D, since $J_n = \mu q' E'$. Therefore, the value of M changes in proportion to μ. It is confirmed that M/μ is constant (as shown by a scale on the right-side vertical axis in Fig. 5), by comparing the value for μ = 1000, 2000, 4000, and 8000 $cm^2/V \cdot s$, respectively. The carrier density and frequency by which the value of M becomes a peak are in a transient region where the propagation velocity changes and the attenuation forms a peak. This fact is shown more clearly by comparing Fig. 2 with Fig. 5. It can be summarized that the preferable values of the mobility, carrier density n, and the frequency of an SAW interact with each other, and that the greater the μ the better, while the value of M becomes larger at an appropriate value of the n and f. The value of M increases for a large value of μ, with a small value of the propagation loss (the resistance loss related to the current caused by the movement of the carriers).

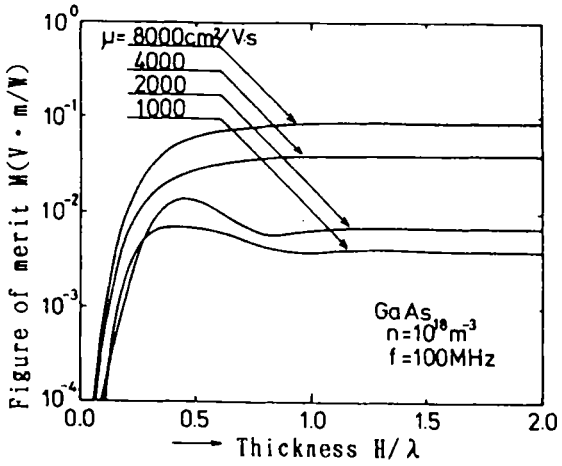

Fig. 6. Figure of merit vs. thickness with mobilities as a parameter.

2.3 Structure of the SAW propagation and the convolver in the double-layer structure

It is assumed that the structure of an epitaxial-growth film on a GaAs semiconductor substrate (S・I・GaAs) is used. The propagation characteristics of a double-layer structure, having a piezoelectric film on a piezoelectric substrate, was analyzed by using the same method as in section 2.1 (i.e., the basic piezoelectric equation is used for the piezoelectric substrate; and Eq. (2) with the semiconductor carrier term for the epitaxial-growth film; then their boundary is connected by the acoustic and electric boundary conditions). The results show that the propagation velocity reduces linearly from 2866.62 m/s for the film thickness ratio H/λ from zero to 0.5; and that the velocity is almost the same as in Fig. 1 for H/λ greater than 0.5. The attenuation increases linearly for H/λ from zero to 0.5; then it becomes constant above H/λ greater than 0.5.

The convolver having a double-layer structure was analyzed by using the same method as in section 2.2. This structure corresponds to that of an epitaxial-growth film on a GaAs semiconductor substrate. Figure 6 shows an example of the results. This shows the dependence of the figure of merit of the convolver on the film thickness, taking the mobility μ as a parameter. When there is no film, the M becomes zero, since there is no nonlinear current. When the film becomes thicker, M approaches the figure of merit of the film alone. The propagation velocity of the SAW, as the attenuation value, becomes almost the same as the value for the film alone, when the film thickness is almost equal to one wavelength.

Table 2. Substrate for GaAs liquidus growth

Type	Si dope n-type
Carrier density	$1.0 \times 10^{24}/m^3$

Table 3. Characteristics of a liquidus-growth GaAs layer

Type	n-type undope
Carrier density	$2.4 \times 10^{20}/m^3$
Resistivity	$6.5\Omega \cdot cm$
Electron mobility	$4000\ cm^2/V \cdot s$
Thickness of L.P.E. layer	17 μm

At a particular film thickness, the greater the mobility μ, the greater the figure of merit *M*.

Table A1 (Appendix) shows the constants used for the numerical analysis in section 2.

3. Experiments of a GaAs Convolver

Various structures of GaAs substrates have been reported for the SAW. In the use of a semiconductor doped with Cr and O, the piezoelectricity of GaAs itself is utilized. A type using GaAs with epitaxial-growth film which utilizes the interaction of the surface wave on the semiconductor was published [6]. Other types using GaAs with ZnO piezoelectric film (since the piezoelectricity of GaAs is small) [7, 8]; and a type with SiO_2 substrate (for improving the temperature characteristic) [2] have been published. Convolvers and correlators which utilize the nonlinear characteristics have been studied as signal-processing devices.

The analyses in sections 2.2 and 2.3 show that a GaAs substrate having the carrier density of $10^{18}/m^3$ is best for obtaining a large figure of merit *M*. However, present technology does not achieve this standard. Thus, an experiment was carried out which controls the carrier density by depleting it with a bias voltage. To obtain the carrier density of the order of $10^{18}/m^3$ by a bias voltage and a sufficiently thick depletion layer, it is necessary to make the impurity n_B small. Therefore, a liquidus-growth film is used. To apply the bias voltage efficiently to the depletion, a substrate for the growth having a large carrier density (N_-/N_+ substrate) was used in the experiment.

Table 4. Dimensions of I.D.T. electrode

Period of electrode	18.8 μm
Width of electrode	4.7 μm
Aperture width cross. part	2.2 mm
Number of pairs	50

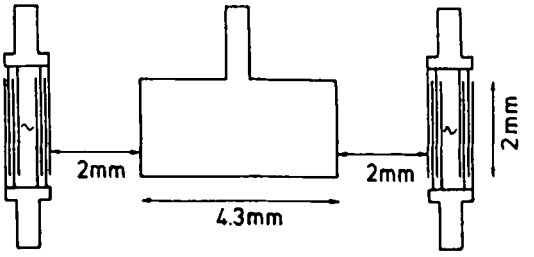

Fig. 7. Configuration of convolver electrode.

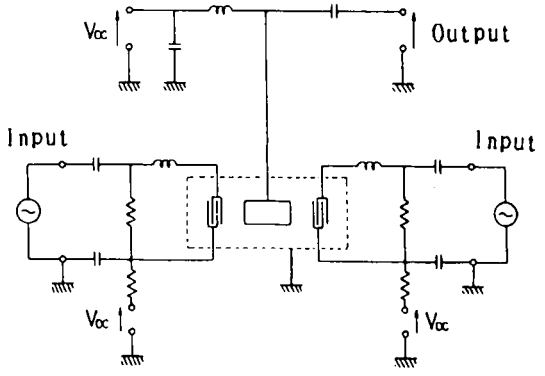

Fig. 8. Measurement circuit of GaAs convolver.

3.1 Fabrication of a convolver specimen

Tables 2 and 3 show the characteristics of the convolver with the n-type GaAs substrate used for the experiment. Table 4 shows the dimensions of the Inter-Digital Electrode (I.D.T). The central frequency of this device is about 155 MHz.

Figure 7 shows the configuration of the convolver element. In this configuration,

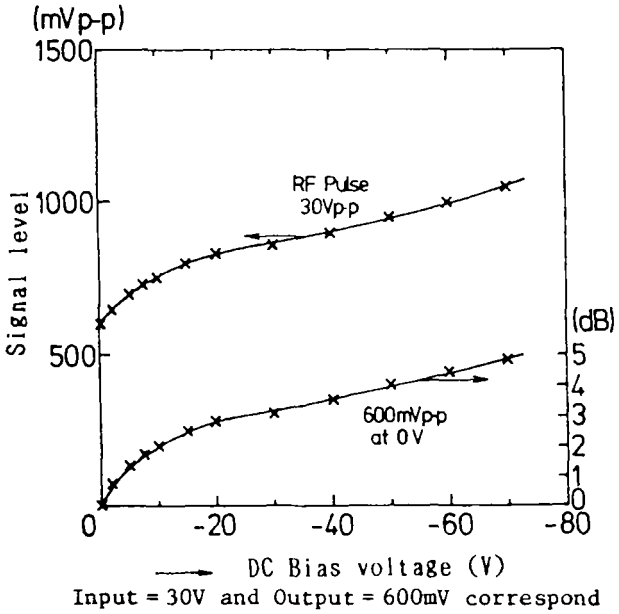

Input = 30V and Output = 600mV correspond to 0 dB.

Fig. 9. Signal level vs. dc bias voltage of I.D.T.

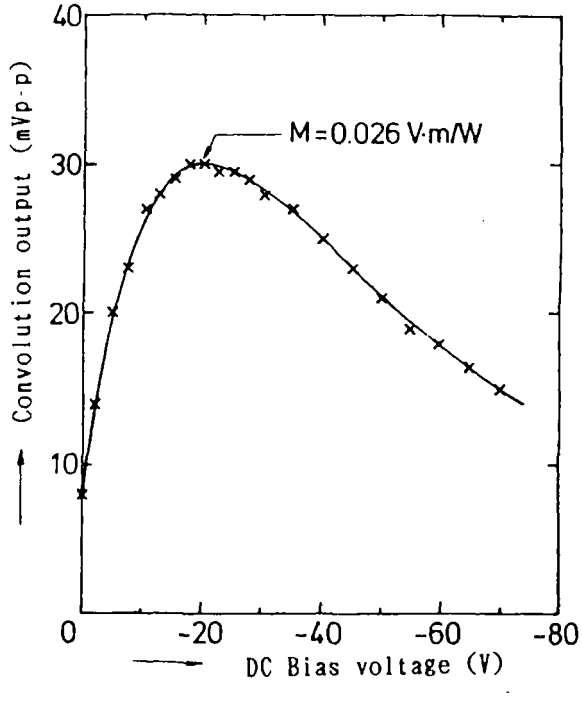

Fig. 10. Convolution output vs. dc bias voltage of output electrode.

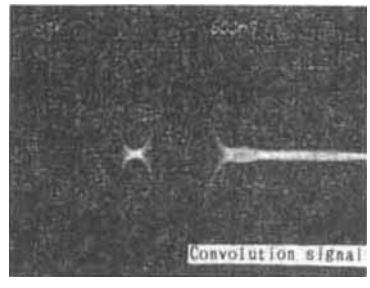

Fig. 11. Convolution output waveform.

the interaction time is 1.5 μs at the interaction length of 4.3 mm.

It is not easy, considering from the analysis in section 2, to excite the SAW on the n-type undoped GaAs film by using the I.D.T. electrode. This is because this device has large carrier density and the difference of velocities at the electrically open and short-circuited surface is small.

The convolver output of the above-described device is considered to be small. Therefore, the measurement of the output is carried out by making the I.D.T. electrode and the convolver output electrode in a Schottky structure, and by reducing the carrier density with a dc bias. Thus, the electromechanical coupling coefficient K^2 becomes large [9].

3.2 Experiment of a GaAs convolver

Figure 8 shows the dc-voltage applying circuit used for the measurement of the GaAs convolver. Figure 9 shows the change of the convolver output due to the dc bias voltage when the SAW is sent and received by the two I.D.T. electrodes. A deep impurity of the impurity density n_B of the LPE layer of the GaAs can be taken as $n_B \simeq 10^{21}\mathrm{m}^{-3}$ which is greater than the carrier density n by one order. Then a breakdown voltage V_B = 100 V is obtained. The thickness of the depletion layer is about 15 μm in this condition, and the layer covers the entire LPE layer. Since the wavelength of the SAW is about 19 μm at the frequency of 155 MHz in the experiment, the electromechanical coupling coefficient K^2 is considered to be almost equal to that of the semiinsulating substrate. Figure 9 shows that the increase of the signal level by about 5 dB at the bias voltage V_B = 70 V. For the input voltage V_{pp} = 30 V, however, the change of the insertion loss is as small as about 2 dB, even with the bias voltage V_B = 0. This is because the same effect as applying the bias is caused automatically by the rectifying effect of the GaAs. In the measurement of the characteristics of the convolver which applies a high input voltage, the bias voltage V_B for the I.D.T. electrode

was set at zero. When $V_B = 0$, the convolution effect is small, since the carrier density in the GaAs is too large. On the other hand, when V_B is too large, the carrier density becomes too small. Then the convolution effect becomes low, the maximum value being $M = 0.026$ V · m/W around $V_{BC} \approx -20$ V. This agrees with the numerical analysis shown in Fig. 4. The insertion loss of the I.D.T. in this condition was about 16 dB per transducer. Figure 11 shows the output waveform of the convolution under this condition. This figure shows that the triangle-shaped convolution output waveform has twice the frequency of the input square wave (i.e., about 310 MHz).

4. Conclusions

In this paper, the propagation characteristics of the SAW on a piezoelectric semiconductor (a piezoelectric element with semiconductor carriers) was analyzed, and the changes of the velocity and attenuation of the SAW due to the mobility and carrier density were found. The nonlinear current under these conditions was obtained from the distribution of displacements of the SAW. Then the figure of merit of the convolver was obtained. These show that it is possible to obtain a relatively large figure of merit with a small attenuation even for a GaAs having a small electromechanical coupling coefficient. The calculated figure of merit was 7×10^{-2} V · m/W which is comparable with that of a practical convolver having an $Si/LiNbO_3$ structure [10]. Since the convolver has a monolithic structure, it is advantageous in that a uniform coupling coefficient can be obtained along a long interaction length.

A convolver with an n-type substrate was fabricated and measured. It was confirmed that the insertion loss can be improved by using a dc bias in a GaAs substrate with Schottky electrode structure. Experiments with the convolver show a good agreement with the theory. We wish to develop this study further for the improvements of the insertion loss by using, for example, ZnO film for the I.D.T. electrode; and realization of a high-efficiency convolver by making a substrate which has an optimum current density of a GaAs growth layer.

REFERENCES

1. G. S. Kino. Acoustoelectric Interactions in Acoustic-Surface-Wave Devices. Proc. IEEE, 64, p. 724 (May 1976).
2. T. W. Grudkowski, G. K. Montress, M. Gilden and J. F. Black. GaAs Monolithic SAW Devices for Signal Processing and Frequency Control. Proc. Ultrasonics Symposium, p. 88 (Nov. 1980).
3. A. R. Hutson and D. L. White. Elastic Wave Propagation in Piezoelectric Semiconductors. J. Appl. Phys., 33, p. 40 (Jan. 1962).
4. I. A. Victorov. Rayleigh Waves in Gallium Arsenide Semiconductor Piezoelectric Crystals. Soviet Physics-Doklady, 14, p. 660 (Jan. 1970).
5. K. Yamanouchi, Y. Cho and T. Inada. $InSb/LiNbO_3$ structure surface-acoustic-wave nonlinear device. The Record of Electrical and Communication of Engineering Conversazion, Tohoku University, 51-2 (1980).
6. S. Ludvik and C. F. Quate. Nonlinear Interaction of Acoustic Surface Waves in Epitaxial Gallium Arsenide. Electronics Letters, 8, p. 551 (Aug. 1972).
7. G. R. Adams, J. D. Jackson and J. S. Hecks. Monolithic ZnO-GaAs Acoustoelectric Devices. Proc. Ultrasonics Symposium, p. 109 (Nov. 1980).
8. K. Kuroda, K. Kyuma, M. Nunoshita, and T. Nakayama. Analysis of the propagation characteristics of surface acoustic waves on a ZnO/GaAs structure. Nihon Gakujutsu Sinkokai, the 131st Committee, SAW-device Subcommittee, Research Data, p. 9 (Jan. 1983).
9. S. Takada, H. Hayakawa, T. Ishiguro and N. Mikoshiba. Depletion-Layer Transduction of Surface Waves on Piezoelectric Semiconductor. Japan. J. Appl. Phys., 11, p. 24 (Jan. 1972).
10. O. W. Otto. Theory for nonlinear coupling between a piezoelectric surface and an adjacent semiconductor. J. Appl. Phys., 45, p. 4373 (Oct. 1974).

APPENDIX

Table A1. Material constants of GaAs

Crystal group	$\bar{4}3m$
Elasticity constants c_{11}^E ($\times 10^{11}$ N/m^2)	1.19
c_{12}^E	0.538
c_{44}^E	0.595
Piezoelectric constant e_{14} (C/m)	−0.160
Dielectric constant $\varepsilon_{11}^S/\varepsilon_0$	11.0
Density ρ ($\times 10^3$ kg/m^3)	5.31